HEAT EXCHANGERS DESIGN AND WORKING FLUID SELECTION FOR AN ORGANIC RANKINE CYCLE

Mădălina Irina GHILVACS[1], Tudor PRISECARU[2], Horaţiu POP[2], Valentin APOSTOL[2], Mălina PRISECARU[2], Cristina CIOBANU[2], Elena POP[2], Hamzath MOHANAD[2]

Among other technologies the organic Rankine cycle (ORC) can be used to recover waste heat from an internal combustion engine (ICE). This paper describes the performance of exhaust heat recovery using an ORC in a passenger car. The heat transfer properties are evaluated over the engine's entire operating region based on the measured data. Subsequently, a mathematical model of the plate heat exchangers is created based on the specific ORC working conditions. The main aims of this study are 1) the determination of the proper working fluid for ORC system, and 2) the calculation of the heat transfer coefficient and the required surface area for the plate heat exchangers (evaporator and condenser).

Keywords: plate heat exchanger, diesel engine, waste heat recovery, organic Rankine cycle, heat transfer coefficient.

1. Introduction

Energy savings and efficiency improvements of energy system are an important task on the path towards a more sustainable future. The efficiency of an internal combustion engine refers to the percentage of the energy resulting from the combustion that actually is applied to moving the car or running the accessories. For current ICEs, the proportion of fuel energy converted into effective work at medium and high loads is about 30% - 45% for the diesel engine or 20% - 30% for the gasoline engine, and the rest is mainly brought into the environment by the exhaust gas and cooling system. ORC is considered a way of converting this waste heat into electrical energy. Several studies have examined Rankine cycles for exhaust gas heat recovery in vehicle applications [1-3]. In this study, the heat transfer characteristics of the evaporator and condenser were analyzed using measured data such as exhaust gas mass flow rate and exhaust gas temperature. This study concerns plate heat exchangers (PHEs) because of their compact construction, ease of cleaning, flexibility of altering the thermal size, pure counter-current flow operation, and high heat transfer efficiency per unit volume.

[1] PhD Stud., University POLITEHNICA of Bucharest, e-mail: make_madalina@yahoo.com
[2] University POLITEHNICA of Bucharest, Splaiul Independenţei 313, Bucharest, Romania.

2. System description

In this study, a commercial engine applied in vehicles was used for heat recovery. This is a 1.5 liter, compression ignition, four-cylinder engine with linear arrangement [4].

The ORC is a vapor power cycle used in numerous applications to generate electrical power. Figure 1 shows a schematic of a simple ORC. It is composed by four main components: a pump, an evaporator, a turbine/generator and a condenser.

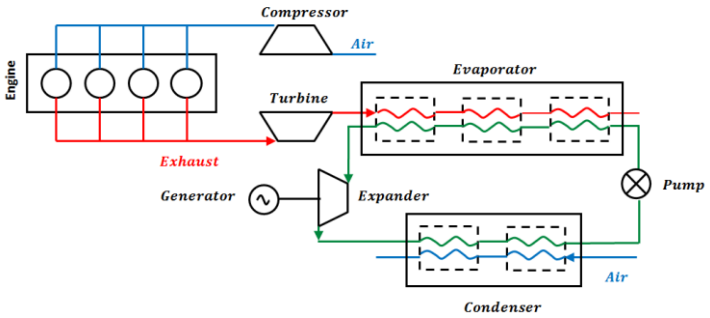

Fig. 1. Schematic of an ORC for engine exhaust heat recovery

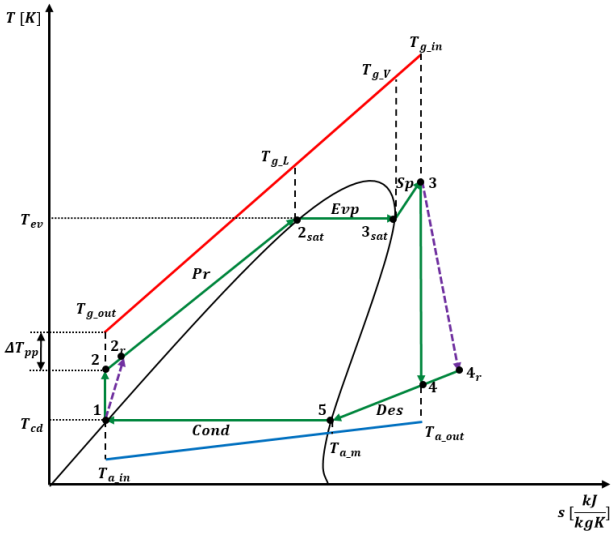

Fig. 2. T–s diagram of the ORC

The associated T–s diagram of the ORC is described in figure 2. The ideal thermodynamic cycle includes the following processes: an isentropic compression process in a pump (1-2), an isobaric heat transfer process in an evaporator (2-3), an isentropic expansion process through a turbine (or other expansion machine) (3-4), and an isobaric heat transfer process in a condenser (4-5-1).

The performance of the Rankine cycle depends on the heat exchanger's effectiveness as well as the pump and expander selection. The approach used in this work draws inspiration from the work of Vargas et al. [5] where the evaporator is assumed to be divided into three sub-segments "a preheater, a boiler and a superheater" linked in series and the condenser is split into two virtual zones corresponding to the state of the working fluid [6] i.e. two phase and gas phase.

3. Mathematical modeling

Before create the mathematical model of this system to simplify the analysis, some general assumptions are formulated as follows:

- Steady-state and steady-flow condition;
- No pressure drops in heat exchangers and connecting pipes;
- The condenser temperature is assumed to be 45 °C;
- Exhaust gas temperature at the exit of evaporator is 140 °C due to prevent condensation of components;
- The expander mechanical efficiency, η_D = 70%;
- The efficiency of the pump, η_P = 80%;
- Ambient temperature is 20 °C;
- Heat exchanger effectiveness η_{PHE}=1.

The flow chart of the program is presented in figure 3. After we chose the working fluid, the mass flow rate of the working fluid and the heat transfer rates for all zones are computed according to energy equation. Subsequently, the convective heat transfer coefficients of each zone are calculated according to the heat transfer correlations and the thermodynamic properties of the exhaust gas and working fluid on each side. Furthermore, the overall heat transfer coefficient of each zone is obtained. Then, the heat transfer area required for each zone is determined using the logarithmic mean temperature difference (LMTD) method.

The total heat transfer rate between the counter flows in plate heat exchangers can be calculated as follows:

$$\dot{Q}_{pr} = \dot{m}_{ref}\left(h_{2sat} - h_2\right) = \dot{m}_{gas} C_{Ppr}(t_{gL} - t_{gasout}) \quad (1)$$

$$\dot{Q}_{vap} = \dot{m}_{ref}\left(h_{3sat} - h_{2sat}\right) = \dot{m}_{gas} C_{Pvap}(t_{gV} - t_{gL}) \quad (2)$$

$$\dot{Q}_{sî} = \dot{m}_{ref}\left(h_3 - h_{3sat}\right) = \dot{m}_{gas} C_{Psî}(t_{ga\sin} - t_{gL}) \quad (3)$$

$$\dot{Q}_{des} = \dot{m}_{ref}\left(h_4 - h_5\right) = \dot{m}_{aer} C_{Paer}(t_{aout} - t_{amed}) \quad (4)$$

$$\dot{Q}_{cond} = \dot{m}_{ref}\left(h_5 - h_1\right) = \dot{m}_{aer} C_{Paer}(t_{amed} - t_{ain}) \quad (5)$$

The logarithmic mean temperature difference can be obtained from the basic counter flow LMTD equation:

$$\Delta T_m = \frac{\Delta T_{\max} - \Delta T_{\min}}{\ln \frac{\Delta T_{\max}}{\Delta T_{\min}}} \tag{6}$$

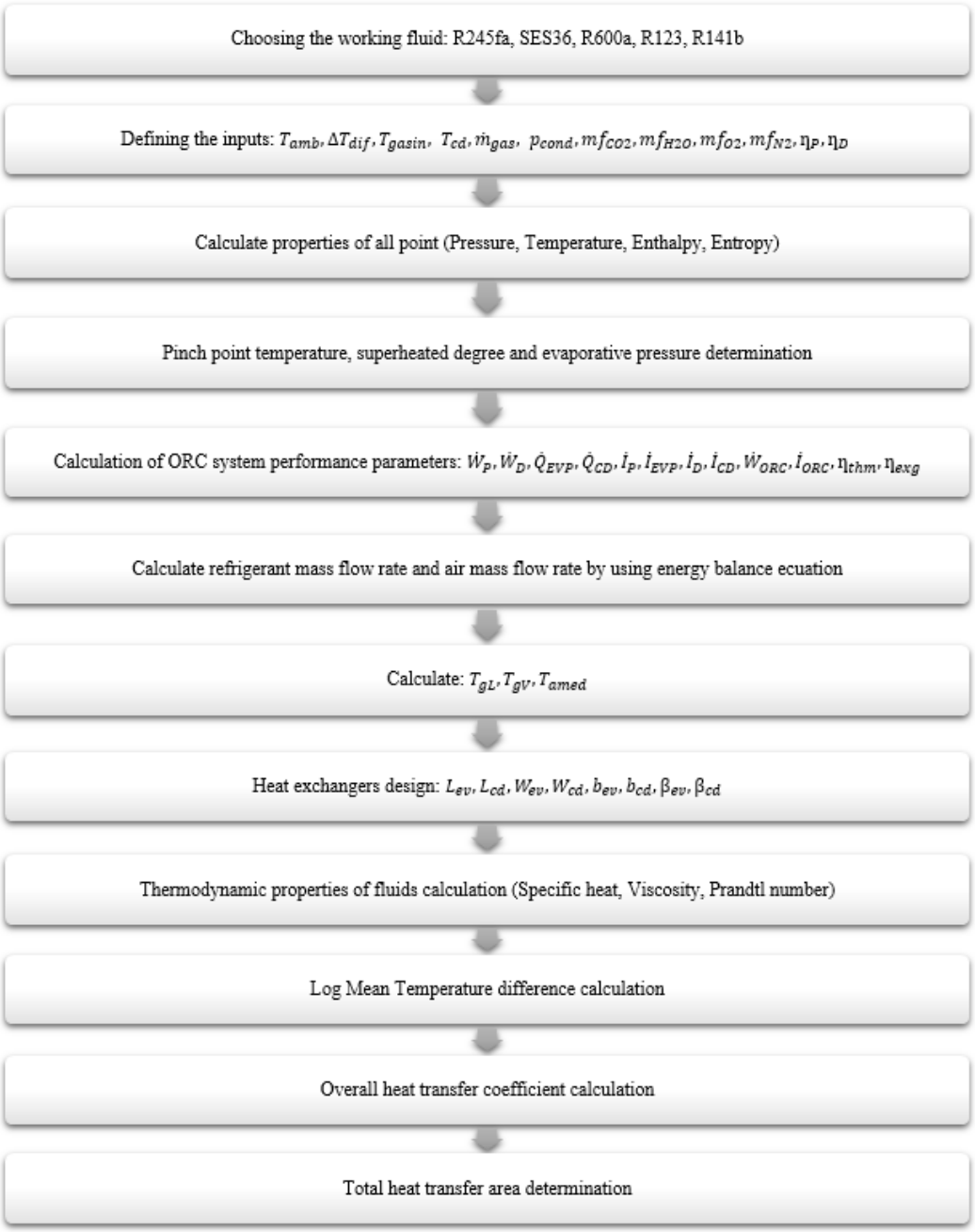

Fig. 3. Flow Chart of program

The system performance parameters (absorbed heat, rejected heat, ORC thermal efficiency, net power, exergy destruction rate and exergy efficiency) have been previously studied [7, 16].

The phase-change heat transfer process generally has three stages in which the heat transfer coefficient abides by different correction equations: liquid phase stage, two phase stage and vapor phase stage. The heat transfer processes for single-phase flow and two-phase flow are respectively discussed below.

In the single phase flow zone, both for liquid and vapor, the heat transfer coefficient is widely predicted by Chisholm and Wanniarachchi correlation.

The overall heat transfer coefficient is given by:

$$\frac{1}{U_m} = \frac{1}{\alpha_C} + \frac{\delta}{\lambda} + \frac{1}{\alpha_H} \tag{7}$$

The Chisholm and Wanniarachchi correlation is employed to calculate the Nusselt number for both hot fluid and cold fluid, which is a function of the Reynolds, Prandtl numbers and the chevron angle of the plates [11]:

$$Nu = 0.724\left(\frac{6\beta}{\pi}\right)^{0.646} \mathrm{Re}^{0.583}\,\mathrm{Pr}^{1/3} \tag{8}$$

The Reynolds number is given by

$$\mathrm{Re} = \frac{GD_h}{\eta} \tag{9}$$

$$G = \frac{\dot{m}}{N_{ch} bW} \tag{10}$$

The number of channels for the hot and cold sides in plate heat exchangers could be calculated respectively as:

$$N_{ch\_H} = \frac{N_{PHE}}{2} \tag{11}$$

$$N_{ch\_C} = \frac{N_{PHE} - 2}{2} \tag{12}$$

$$N_{PHE} = N_{ch\_C} + N_{ch\_H} + 1 \tag{13}$$

The hydraulic diameter D_h is expressed as the ratio of four times the flow channel cross sectional area to the wetted perimeter [12].

$$D_h = \frac{4A}{P} = \frac{4[bw]}{2[b+w]} = 2b \tag{14}$$

$$\mathrm{Pr} = \frac{C_p \eta}{\lambda} \tag{15}$$

The convection heat transfer coefficient for single-phase flow is:

$$\alpha = \frac{\lambda Nu}{D_h} \tag{16}$$

In the two-phase region (condensation or evaporation), the fluid properties such as density, specific heat, viscosity and thermal conductivity are observed to suffer from dramatic variations with the quality variation of organic working fluid. For this reason the heat transfer process in the two-phase region is divided into relatively small sections, with so slight property variations in each section that constant properties can be assumed.

The overall heat transfer coefficient for each section is given by

$$\frac{1}{U_{b(i)}} = \frac{1}{\alpha_{C(i)}} + \frac{\delta}{\lambda} + \frac{1}{\alpha_{H(i)}} \tag{17}$$

Specifically for the evaporating process, Nusselt number is calculated using Yan and Lin's correlation. The evaporation heat transfer coefficient on the cold side for each section in evaporator is expressed as [13]:

$$\alpha_{evp(i)} = \frac{Nu_{C(i)}\lambda_i}{D_h} \tag{18}$$

$$Nu_{C(i)} = 1.926\,\mathrm{Pr}_l^{1/3}\,Bo_{eq(i)}^{0.3}\,\mathrm{Re}^{0.5}\left[1 - x_i + x_i\left(\frac{\rho_l}{\rho_v}\right)^{0.5}\right] \tag{19}$$

For the condensation process, Nusselt number is calculated using Yan's correlation. The condensation heat transfer coefficient is expressed as [14]:

$$\alpha_{cond(i)} = \frac{Nu_{H(i)}\lambda_i}{D_h} \tag{20}$$

$$Nu_{H(i)} = 4.118\,\mathrm{Re}_{eq(i)}^{0.4}\,\mathrm{Pr}_l^{1/3} \tag{21}$$

$$\mathrm{Re}_{eq(i)} = \frac{G_{eq(i)}D_h}{\eta_l} \tag{22}$$

$$Bo_{eq(i)} = \frac{q}{G_{eq(i)}r_{ev}} \tag{23}$$

$$G_{eq(i)} = G\left[1 - x_i + x_i\left(\frac{\rho_l}{\rho_v}\right)^{0.5}\right] \tag{24}$$

Then, the heat transfer area for each zone is calculated as follows:

$$A_j = \frac{\dot{Q}_j}{U_j \Delta T_{m\_j}} \tag{25}$$

Where $j = pr, sî, vap, des, cond$

4. Results analysis

A program was created to evaluate the evaporator and condenser performance in Engineering Equation Solver (EES) according to the established mathematical model.

Tabel 1

The basic properties of the selected working fluids

No.	Working fluid	Type of fluid	t_{cr} [°C]	p_{cr} [bar]	ODP	GWP_{100}	Safety group classification
1	R245fa	Isentropic	154	36.4	0	1030	A1
2	SES36	Dry	177.5	28.49	0	3126	A1
3	R123	Isentropic	184	36.6	0.06	93	B1
4	R600a	Dry	152	37.96	0	3	A3
5	R141b	Isentropic	204.2	40.6	0.11	630	A2

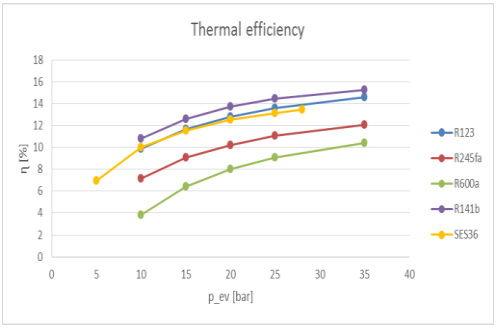

Fig. 4. Variation of thermal efficiency with evaporating pressure

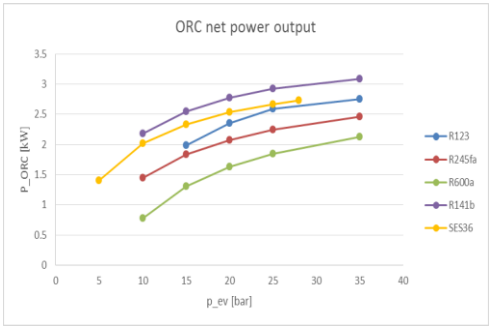

Fig. 5. Variation of net power output with evaporating pressure

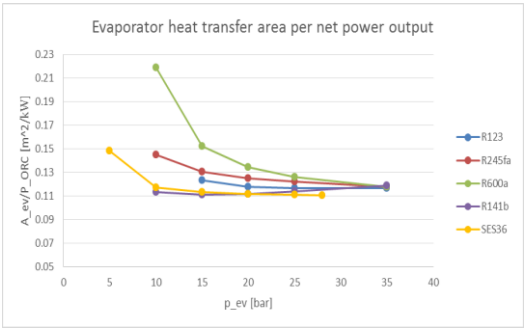

Fig. 6. Variation of evaporator heat transfer area per net power output with evaporating pressure

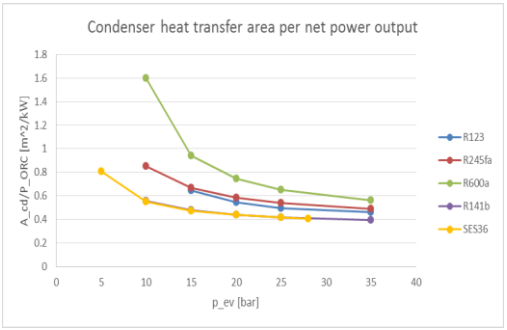

Fig. 7. Variation of condenser heat transfer area per net power output with evaporating pressure

The first step in the design procedure of an ORC system is the selection of the organic fluid. To select an appropriate working fluid to achieve the maximum thermal efficiency and exergy efficiency in various working conditions, a preliminary selection was conducted. In addition, material compatibility,

flammability, toxicity, global warming potential (GWP), Ozone depletion potential (ODP) and other properties also need to be considered when selecting working fluids. Based on these considerations five working fluids are used in the present study, their basic physical parameters are shown in table 1.

The net power output of the ORC and its thermal efficiencies can be written as follows:

$$\dot{W}_{ORC} = \dot{m}_{ref}(h_3 - h_4) - \dot{m}_{ref}(h_2 - h_1) \tag{26}$$

$$\eta_{thm} = \frac{\dot{W}_{ORC}}{\dot{Q}_{EVP}} \tag{27}$$

Where: $\dot{m}_{ref}$ is the mass flow rate of the working fluid, h_1, h_2, h_3 and h_4 are the enthalpies of four specific points as shown in figure 2, $\dot{W}_{ORC}$ is the net power output of the ORC, η_{thm} is the thermal efficiency of the ORC.

Figures above show the performances of working fluids investigated for the ORC system on following criteria: thermal efficiency, net power output and total heat transfer area per net power output. Comparing the highest thermal efficiency value presented by each fluid, R141b is the highest one of about 15.25% at evaporating pressure 3.5 MPa, followed by R123 (14.75%, 3.66 MPa) > SES36 (13.53%, 2.85 MPa) > R245fa (12.22%, 3.64 MPa) > R600a (10.53%, 3.62MPa).

As shown in figure 5, ORC net power value is increasing as the increase of evaporating pressures. The increase trend of various working fluids is obvious at low evaporating pressures and becomes smooth near critical pressure. Among all the considered working fluids, R141b presents the highest net power value of about 3.089 kJ/kg at evaporating pressure 3.5 MPa.

Table 2

Input parameters for plate heat exchangers

	Plate height	Plate width	Channel space	Corrugation angle
Evaporator	0.2 [m]	0.1 [m]	0.004 [m]	60°
Condenser	0.35 [m]	0.21 [m]	0.004 [m]	60°

It is noted that lower heat transfer area per net power output value expresses that smaller total heat transfer areas would be needed in order to achieve the same net power output which can indicate the heat transfer performance and reduce the system investment in some aspect [9]. As we can see form figures 6 and 7, SES36 and R141b show the lowest values.

As a results, the R141b show the best performance for the ORC system, but if we are considering the environmental characteristics (ODP value <0.20 and GWP value < 1500), the R245fa will be chosen as working fluid for our study.

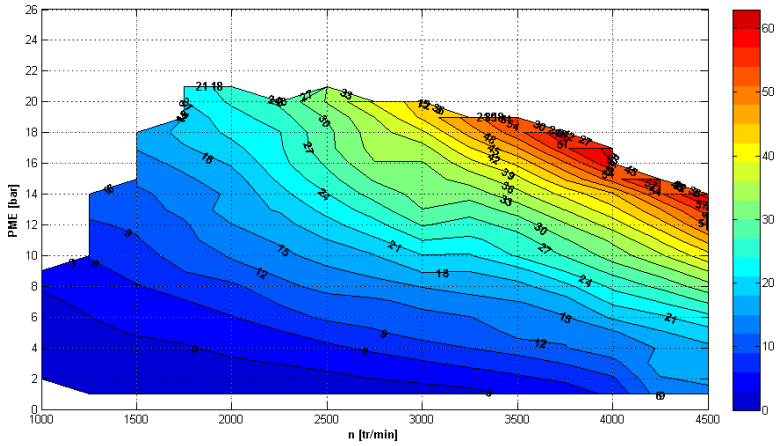

Fig. 8. Heat transfer rate variation in evaporator [kW]

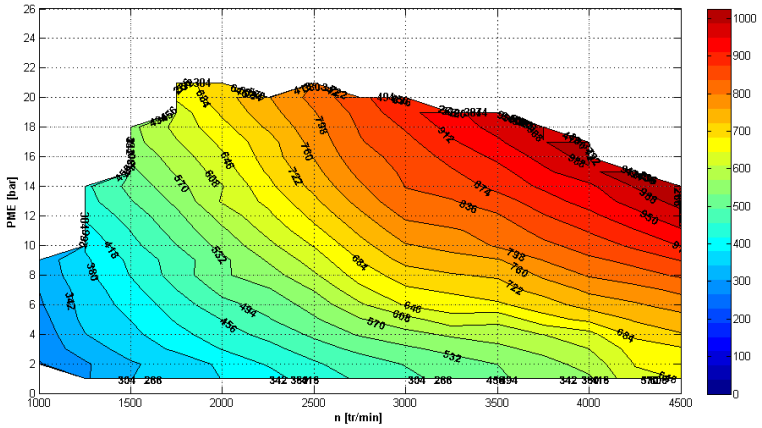

Fig. 9. Overall heat transfer coefficient variation in boiler [W/m^{2}K]

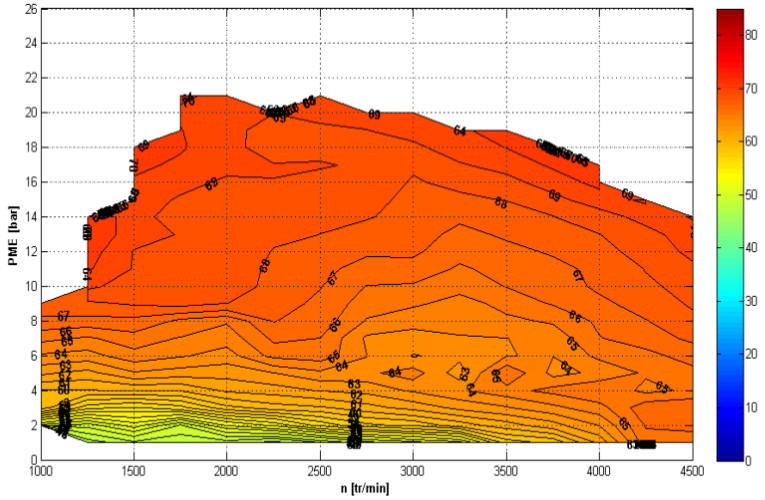

Fig. 10. Heat transfer area for preheated zone [%]

To evaluate the plate heat exchangers performance, we first obtain the waste heat quantities of the exhaust of the diesel engine [7]. The variation of the heat transfer rate for evaporator accordingly with entire engine's operating region is presented in figure 8. This variation characteristic is similar to that of the engine power because the waste heat energy provided by the exhaust gas increases with engine power. At the rated power point, the overall heat transfer rate reaches 60 kW.

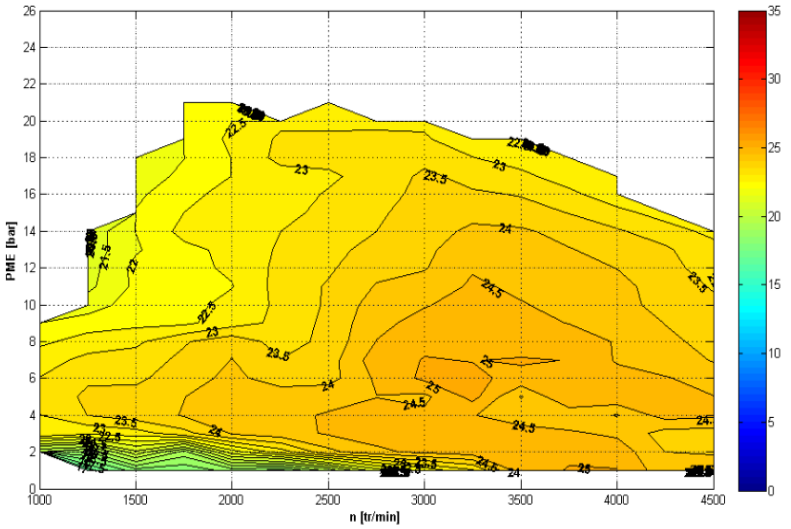

Fig. 11. Heat transfer area for two-phase zone [%]

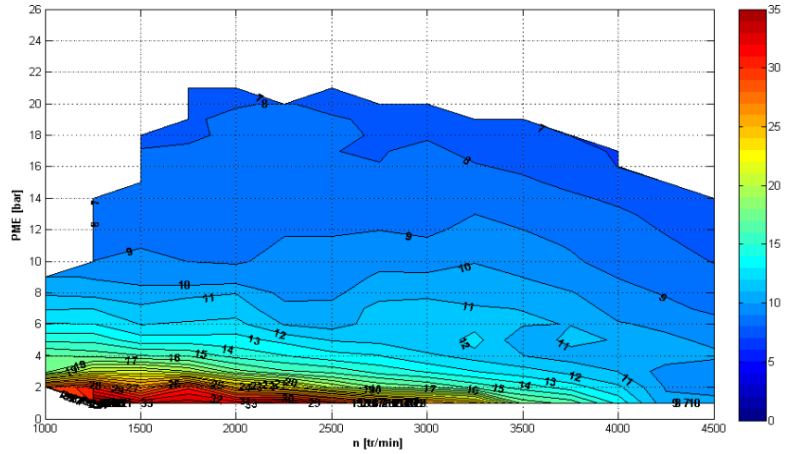

Fig. 12. Heat transfer area for superheated zone [%]

The values of the overall heat transfer coefficient depend on the heat transfer coefficient on the both hot and cold side. Figures 9 show the overall heat transfer coefficient variation in boiler over the entire engine`s operation region. As we can see the overall heat transfer coefficient value increases with engine speed and engine load.

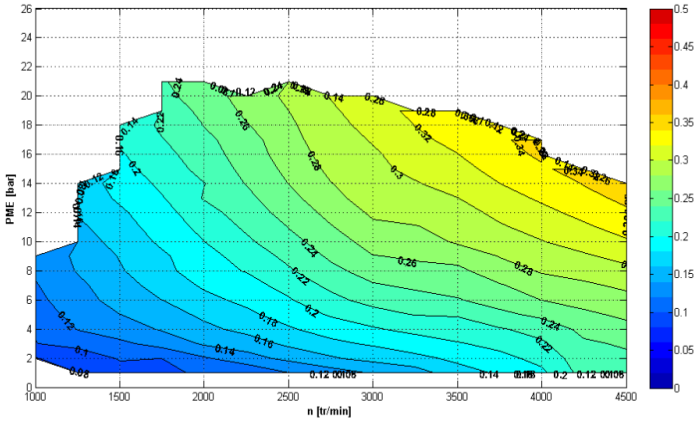

Fig. 13. Overall heat transfer area for evaporator [m^2]

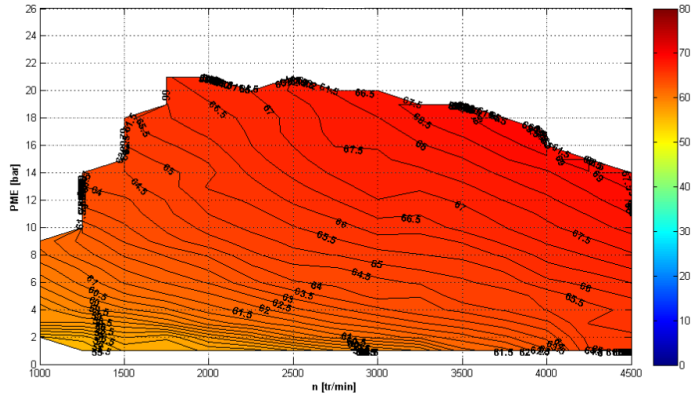

Fig. 14. Heat transfer area for two-phase zone in condenser [%]

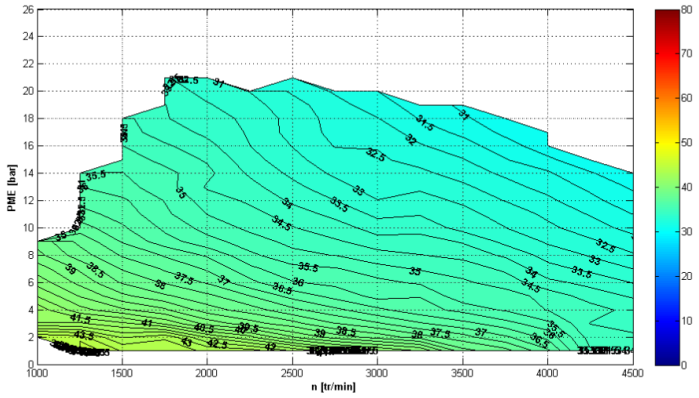

Fig. 15. Heat transfer area for desuperheater zone [%]

The heat transfer area required for each zone is calculated using the LMTD method, figures 10 -16. At the rated power point, the heat transfer areas of evaporator and condenser are 0.35 m^2, and 2.15 m^2, respectively. The area of preheater and boiler zones is increase with engine speed and engine load while the area of superheater is decrease with engine speed and engine load. The percentage

area for preheater zone is approximately 67% from total evaporator area, while for boiler zone is 23% and for superheater zone is 10 %. The desuperheater heat transfer area is almost 35% from condenser area.

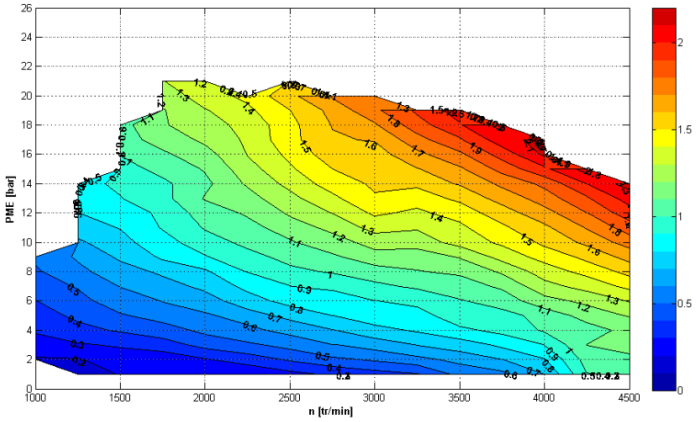

Fig. 16. Overall heat transfer area for condenser [m^2]

5. Conclusions

This paper presents the effects of different working fluids on the performance of organic Rankine cycle used for automotive exhaust waste heat recovery. The performance and thermal efficiency of the ORC system are affected by working fluid significantly, because the thermodynamic and heat transfer properties vary for each working fluid. Although R141b had the highest net power output, R245fa was chosen as a better suited fluid for our system mainly due to its non-flammable behavior and thermodynamic performance.

Our analysis includes also the evaluation of heat transfer area for the appropriate heat exchangers over the engine`s entire operation region. The overall heat transfer rate increases with engine speed and engine load. Furthermore, the heat transfer rate of each zone is proportional to that of the overall heat transfer rate when the engine operating condition changes. The heat transfer area of the preheated zone is the largest, which is more than half of the total area. The heat transfer area of the two-phase zone is slightly greater than that of the superheated zone primarily caused by the discrepancies of the heat transfer rates.

Acknowledgements

The present work has been supported by the Romanian government through Research grant," Hybrid micro-cogeneration group of high efficiency equipped with an electronically assisted ORC", 2nd National Plan, Grant Code: PN-II-PT-PCCA-2011-3.2-0059, Grant No.: 75/2012.

Nomenclature

Nomenclature			**Subscript**	
Symbol	**Definition**	**Unit**	**Symbol**	**Definition**
A	Area	[m^2]	*a, aer*	Air
b	Channel spacing	[m]	*amb*	Atmospheric
Bo	Boiling number	[-]	*b*	Two-phase region
c_p	Specific heat	[J/kgK]	*C*	Cold fluid
D	Diameter	[m]	*CD, cond*	Condenser
G	Mass flux	[kg/m^2s]	*ch*	Channel
h	Enthalpy	[kJ/kg]	*cr*	Critical
$\dot{I}$	Exergy destruction rate	[kW]	CO_2	Carbon dioxid
L	Plate length	[m]	*D*	Detentor, Expander
$\dot{m}$	Mass flow rate	[kg/s]	*Des*	Desuperheater
mf	Mass fraction	[%]	*Dif*	Difference
Nu	Nusselt number	[-]	*eq*	Equivalent
p	Pressure	[bar]	*exg*	Exergetic
Pr	Prandtl number	[-]	*EVP*	Evaporator
q	Average imposed wall heat transfer rate	[W/m^2]	*g, gas*	Waste heat
Q	Heat transfer rate	[kW]	H_2O	Water
r_{ev}	Enthalpy of vaporization	[J/kg]	*h*	Hydraulic
Re	Reynolds number	[-]	*H*	Hot fluid
t, T	Temperature	[ºC], [K]	*in*	Intel state
ΔT_m	Log mean temperature difference	[grd]	*l, L*	Liquid
U	Overall heat transfer coefficient	[W/m^2K]	*m*	Single-phase region
w	Channel width	[m]	*max*	Maximum
$\dot{W}$	Power	[kW]	*m, med*	Mean
x_i	Vapor quality	[-]	*min*	Minim
			N	Number
			N_2	Nitrogen
			O_2	Oxygen
			out	Outlet state
Greek letters			*P*	Pump
Symbol	**Definition**	**Unit**	*pp*	Pinch point
α	Convection heat transfer coefficient	[W/m^2K]	*pr*	Preheater
β	Chevron angle	[º]	*Ref*	Refrigerant
δ	Thickness	[cm]	*sat*	Saturation
			sî	Superheater
η	Viscosity; Efficiency	[kg/sm], [%]	*PME*	Mean effective pressure
ρ	Density	[kg/m^3]	*thm*	Thermal
λ	Thermal conductivity	[W/mK]	*V*	Vapor

REFERENCES

[1]. *S. E. Aly*, Diesel engine waste-heat power cycle, Applied Energy 29 (1988) 179-189.
[2]. *M. M. Bailey*, Comparative Evaluation of Three Alternative Power Cycles for Waste Heat Recovery Form the Exhaust of Adiabatic Diesel Engines. National Aeronautics and Space Administration, (Washington, DC), 1985.
[3]. *E. Doyle, L. Dinanno, S. Kramer*, Installation of a Diesel Organic-Rankine Compound engine in a class 8 truck for a single-vehicle test, SAE Paper 790646 (1985).
[4] M. I. Ghilvacs, T. Prisecaru, H. Pop, V. Apostol, M. Prisecaru, A. Dobrovicescu, E. Pop, C. Ciobanu, M. H. K. Aboaltabooq, A. Alexandru, A review of low-grade heat recovery using organic Rankine cycle, International symposium ISB-INMA THE, 2015.
[5]. *J. V. C. Vargas, J. C. Ordonez, A. Bejan*, Power extraction from a hot stream in the presence of phase change , International Journal of Heat and Mass Transfer 43 (2000) 191-201 .
[6]. *S. Quoilin, V. Lemort, J. Lebrun*, Experimental study and modelling of organic Rankine cycle using scroll expander, Applied energy, 87(2010)1260-1268.
[7]. *M. I. Ghilvacs*, Assessment of waste heat of internal combustion engines, second report for PhD study, Politehnica University, 2015.
[8]. *H. D. M. Hettiarachchi, M. Golubovic, W. M. Worek, Y. Ikegami*, Optimum design criteria for an organic Rankine cycle using low-temperature geothermal heat sources, Energy 32 (2007) 1698-706.
[9]. *H. Tian, G. Shu, H. Wei, X. Liang, L. Liu*, Fluids and parameters optimization for the organic Rankine cycles (ORCs) used in exhaust heat recovery of Internal Combustion Engine (ICE), Energy 47 (2012) 125-136.
[10]. *H. G. Zhang, E. H. Wang, B. Y. Fan*, Heat transfer analysis of a finned-tube evaporator for engine exhaust heat recovery, Energy Conversion and Management 65 (2013) 438–447.
[11]. *J. R. García-Cascales, F. Vera-García, J.M. Corberán-Salvador, J. Gonzálvez-Maciá*, Assessment of boiling and condensation heat transfer correlations in the modelling of plate heat exchangers, International Journal of Refrigeration 30 (2007) 1029-1041.
[12]. *R. K. Shah, A. S. Wanniarachchi*, Plate heat exchanger design theory in industry heat exchanger, Von Karman Institute for Fluid Dynamics, Belgium, 1992.
[13]. *Y. Y. Yan, T.F. Lin,* Evaporation heat transfer and pressure drop of refrigerant R-134a in a plate heat exchanger, Journal of Heat Transfer 121 (1999) 118-27.
[14]. *Y.Y. Yan, H.C. Lio, T. F. Lin,* Condensation heat transfer and pressure drop of refrigerant R-134a in a plate heat exchanger, International Journal of Heat and Mass Transfer 42 (1999) 993 – 1006.
[15]. *J. Wang, Z. Yan, M. Wang, S. Ma, Y. Dai*, Thermodynamic analysis and optimization of an (organic Rankine cycle) ORC using low grade heat source, Energy 49 (2013) 356-365.
[16]. *M Ghilvacs, T Prisecaru, H Pop, V Apostol, M Prisecaru, E Pop, Gh Popescu, C Ciobanu, A Mohanad and A Alexandru*, Performance analysis of exhaust heat recovery using organic Rankine cycle in a passenger car with a compression ignition engine, 7th International Conference on Advanced Concepts in Mechanical Engineering IOP Publishing, IOP Conf. Series: Materials Science and Engineering 147 (2016) 012147 doi:10.1088/1757-899X/147/1/012147, 2016.